Dynamic Frameworks

DOI: 10.1002/ange.201306304

A Controllable Gate Effect in Cobalt(II) Organic Frameworks by Reversible Structure Transformations**

*Qiang Chen, Ze Chang, Wei-Chao Song, Han Song, Hai-Bin Song, Tong-Liang Hu, and Xian-He Bu**

Materials that show reversible structure transformation and a characteristic response toward specific external stimuli are vitally important for applications in sensing, molecular capture, switches, and so on.[1] In particular, any change of physical properties (such as color, magnetism, and electric resistance) associated with the transformation that could be monitored to indicate the state of these materials, are factors for sensor and other applications. Moreover, owing to the convenience and detail concerning solid-state structure transformation that can be obtained by diffraction methods, single-crystal to single-crystal (SC-SC) structure transformations of crystalline materials have become of importance and interest.[2] In recent years, SC-SC structure transformations of different materials triggered by light,[3] temperature,[4] and guest molecules[5] have been reported. However, SC-SC dynamic structural changes involving breaking and forming of bonds are still rare, particularly for those examples with potential applications.[6]

Herein, we present a reversible SC-SC transformation of Co^{II}-based frameworks induced by coordinative small molecules. A series of changes in structure and physical properties accompanied by the transformation process has been clarified. Particularly, a switchable gate effect was observed in the one-dimensional channels of the frameworks during the transformation process that can be utilized to control the encapsulation and release of guest molecules.

The solvothermal reaction of $CoSO_4{\cdot}7H_2O$, 1,3,5-tris(p-imidazol-ylphenyl)benzene (tipb), and terephthalic acid (H_2pta) in *N*,*N*′-dimethylformamide (DMF) led to the formation of blue block crystals of $[Co_{1.5}(tipb)(SO_4)(pta)_{0.5}]{\cdot}(DMF)_{1.75}$ (**BP**⊃DMF). X-ray crystallographic analysis[7] revealed that in the structure of **BP**⊃DMF there are two crystallographically independent Co^{II} centers involved in the asymmetric unit. Both of the Co^{II} ions are four-coordinate and exhibit tetrahedral coordination geometry, defined by two nitrogen atoms from two independent tipb ligands, and two oxygen atoms from one pta^{2-} ligand and one sulfate anion for Co1 or from two independent sulfate anions for Co2 (Supporting Information, Figure S1a). Tipb ligands link Co^{II} ions to form a bilayer structure (layer b) parallel to the *ab* plane (Supporting Information, Figure S4a). Adjacent layers are connected by sulfate anions along the *c* direction to form a three-dimensional (3D) network (net b; Supporting Information, Figure S5a). Twofold interpenetration of the nets results in rhombic channels along the *c* direction (Supporting Information, Figure S6a). The pta^{2-} ligands located in the channels connect the interpenetrating nets to afford a self-penetrating framework structure (**BP**; Figure 1a). The framework of **BP** reveals 1D ultramicropores along the *c* axis with DMF molecules distributed in the chambers defined by pta^{2-} ligands and channel wall (Figure 3a).

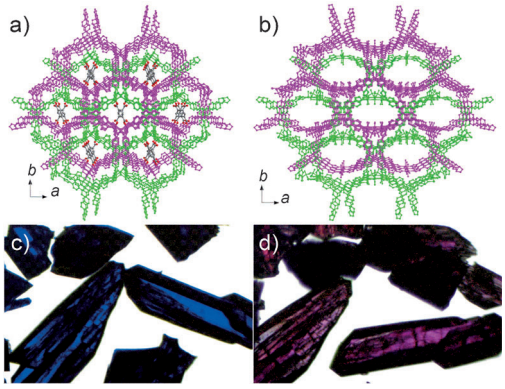

Figure 1. a) Self-penetrating framework of **BP**. b) Twofold interpenetrating framework of **RP**. Microscope image of c) **BP**⊃DMF (blue) and d) **RP**-H_2O (red) crystals.

When **BP**⊃DMF is exposed to air, the blue block crystals gradually turn to red without losing crystallinity. This newly formed red crystal was identified as $[Co_{1.5}(tipb)(SO_4)(H_2O)_{3.6}]{\cdot}(pta)_{0.5}(solvent)_n$ (**RP**-H_2O). X-ray crystallographic analysis of **RP**-H_2O revealed that a SC-SC structural transformation had occurred. In **RP**-H_2O, H_2O ligands displace pta^{2-} ligands and the coordination number of the Co^{II} ions changed from 4 to 6. The coordination configuration of the

[*] Q. Chen, Dr. Z. Chang, Dr. W.-C. Song, H. Song, Dr. T.-L. Hu, Prof. Dr. X.-H. Bu
Department of Chemistry, TKL of Metal- and Molecule-based Material Chemistry and Synergetic Innovation Center of Chemical Science and Engineering (Tianjin)
Nankai University, Tianjin 300071 (China)
E-mail: buxh@nankai.edu.cn
Dr. H.-B. Song
State Key Laboratory of Elemento-Organic Chemistry
Nankai University, Tianjin 300071 (China)

[**] We thank Prof. Jian-Rong Li (Beijing University of Technology), Prof. Michael J. Zaworotko (University of South Florida), and Prof. Wei-Xiong Zhang (Sun Yat-sen University) for the helpful discussions, Dr. Andrey A. Yakovenko (Brookhaven National Laboratory) for the powder refinements, and Hong-Jian Song (Nankai University) for the measurement of NMR spectra. This work was financially supported by the 973 program (2012CB821700), NNSF of China (21031002, 21290171, and 51073079).

Supporting information for this article is available on the WWW under http://dx.doi.org/10.1002/anie.201306304.

Co^{II} ions changed from tetrahedral to octahedral, thus explaining the color changes (Figure 1; Supporting Information, Figure S8). Similar color changes driven by coordination number diversifications have been reported.[6,8] The coordination/torsion angle of tipb ligands (Supporting Information, Figure S1) and relative position of Co^{II} centers (Supporting Information, Figure S2) also changed upon the structural transformation, which bring about only small deformations of the frameworks (Supporting Information, Figures S4–S7). Additionally, the transformation changes the framework from neutral to cationic and the pta^{2-} anions are distributed in the channels randomly to maintain charge balance. Though pta^{2-} ligands were not observed in the crystal structure of **RP**-H_2O (Figure 3b). ^1H NMR spectroscopy, HPLC, and X-ray crystallographic analysis of reversely transformed samples confirmed that pta^{2-} ligands are still in the framework (see the Supporting Information for details). The dissociation of pta^{2-} ligands from the framework makes **RP**-H_2O exhibit micropores along *c* and splits the self-penetrating framework into two interpenetrated identical networks (Figure 1b).

To gain a better visualization and understanding of the structures of **BP** and **RP**, the framework topologies of the complexes were analyzed. With sulfate anions connecting Co_3 clusters and tipb ligands as nodes, the framework of **BP** reveals a new (3,8)-connected self-penetrating topology with a Schläfli symbol of $(4,6^2)_2(4^2,6^{24},8^2)$. **RP** is a twofold interpenetrating (3,6)-connected **sit** net with a Schläfli symbol of $(4,6^2)_2(4^2,6^{10},8^3)$ based on the same simplification (Figure 2).[9] To our knowledge, this is the first example of self-penetrating to interpenetrating topology transformation in a three-dimensional metal–organic framework.

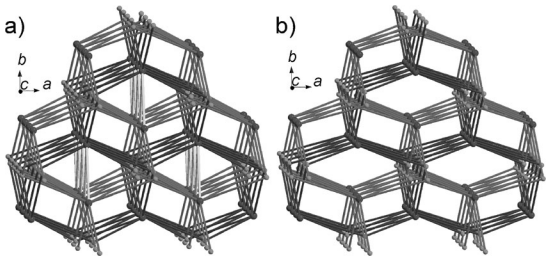

Figure 2. a) The (3,8)-connected self-penetrating topology of **BP**. b) The (3,6)-connected twofold interpenetrating sit topology of **RP**.

By comparing the crystal structures of **BP** and **RP**, the driving force of the structure transformation can be attributed to the presence and coordination of H_2O molecules. This supposition is supported by the observation that the transformation process was accelerated with increased moisture. When **BP** was immersed in water, the transformation process was completed within several minutes (see the Supporting Information for details). Also, the SC-SC transformation was found to be reversible. The coordinated H_2O molecules in **RP** can be removed by heating, vacuum, or immersing the **RP** sample in anhydrous water miscible solvents. By losing the coordinated H_2O molecules, the coordination environment of Co^{II} centers revert to result in **BP** (**BP**-brb), as evidenced by single-crystal diffraction and XRD (Supporting Information, Figure S13, S24). Similar to the **BP** to **RP** process, the reverse transformation process could also proceed rapidly (see the Supporting Information for details). This rapid response and recyclable characteristics are desired for sensing applications, and the associated property change is suitable for the identification and monitoring of the state of targeted system. Furthermore, the structure transformation can also be triggered by the presence of NH_3 (Supporting Information, Figure S14, S15). Based on these characteristics, this material is a good candidate as sensor for these coordinative molecules.[1f,10]

Apart from the investigation of structure transformation, structural analyses of **BP** and **RP** reveal that the dissociation/recovery of pta^{2-} ligands defined two states of the channels, and the role of pta^{2-} ligands, might be described as gates: in **BP**, the coordinated pta^{2-} ligands are ordered in the channels and divide the space in the channels into individual chambers with dimension of about $0.57 \times 0.75 \times 1.9\ nm^3$ (Supporting Information, Figure S18). As the diffusion of guest molecules in the channels blocked by the coordinated pta^{2-} ligands, the state of channels in **BP** could be defined as closed (Figure 3c);

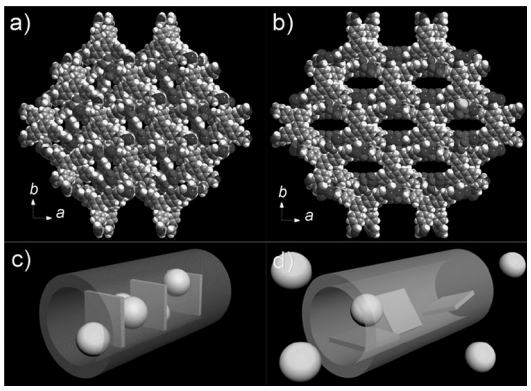

Figure 3. Space-filling view of the crystal structure of a) **BP** and b) **RP** along *c* axis. Schematic diagram of the "gate effect" of the frameworks: c) the gates are closed and guest molecules are sealed, d) the gates are open and guest molecules are released.

in contrast, when **RP** was obtained by structure transformation, the pta^{2-} ligands dissociated from the framework and were dispersed randomly in the channels. These channels are opened, and guest molecules can be released (Figure 3d). Based on the structure transformation investigation, this gate effect should be controllable by the introduction and removal of coordinative molecules.

To confirm the gate effect[11] for controllable guest trapping and release, a pair of tests were designed and performed with DMF molecules as guest (Scheme 1; Supporting Information, Figure S22). The **BP**⊃DMF kept dry remains blue until immersed in D_2O. In D_2O, **BP** turns to **RP** and DMF guests are released (Supporting Information, Figure S22b). In contrast, **BP**⊃DMF kept in a humidistat turns red in about 7 days and releases most of the guest DMF molecules into the air. Almost no DMF could be detected by ^1H NMR (Supporting Information, Figure S22c). This test reveals that the framework of **BP** can effectively encapsulate

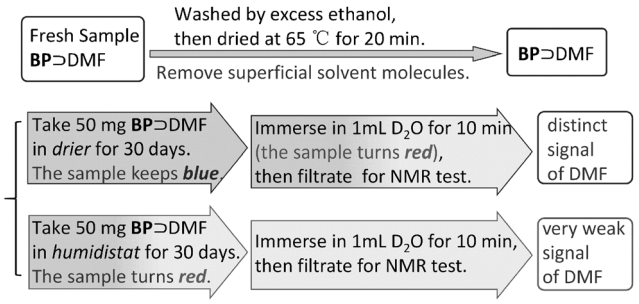

Scheme 1. Contrast test for the confirmation of the gate effect.

DMF molecules and release them in the presence of water vapor (in humidistat) or water (by immersion) by structure transformation. On the other hand, although some of the encapsulated DMF is released when **BP** is immersed in [D_4]MeOH (Supporting Information, Figure S23c), NMR tests reveal that DMF is hardly exchanged by [D_6]DMSO (Supporting Information, Figure S23d). These results indicate that the gate effect in solution could be affected by the properties of solvent. All of the results mentioned above indicate that the structure transformation of the frameworks controls encapsulation and release of small molecules by the gate effect. Moreover, as the color of sample changes with the transformation, the switch state of the gates can be identified and monitored by the color change of the complex.

Apart from DMF, complex **BP** can be synthesized by anhydrous solvents, such as DMAC, DEF, methanol, or ethanol (Supporting Information, Figure S17). These solvent molecules also can be loaded in the chambers of **BP**. Furthermore, these different synthetic methods reduce the cost and toxicity in synthesis.

To further investigate the pore features of the frameworks and confirm the precise condition required for structure transformation, gas and vapor adsorptions were performed. Before the measurements, a sample of **BP**⊃DMF was solvent-exchanged to obtain **BP**⊃CH_3OH (see the Supporting Information for details), and guest methanol molecules were removed by heating under high vacuum to afford guest free **BP**. It should be noted that **RP**-H_2O gradually loses the coordinated and guest H_2O molecules to result in **BP** during the evacuation process, so only **BP** can be tested for gas adsorption. The adsorptions of CO_2, CH_4, and N_2 at 273 K show that **BP** has high adsorption selectivity for CO_2 and CH_4 over N_2 (Figure 4a; see the Supporting Information for details).

Vapor adsorption isotherms of methanol, ethanol, and water for **BP** at 273 K are shown in Figure 4b. For water, the uptake at low pressure is much lower than that of methanol and ethanol. This selective uptake could be attributed to the aromatic, hydrophobic pore surface in **BP**. Surprisingly, the isotherm for H_2O shows a sudden rise between 0.65 and 0.76 mmHg (P/P_0: 0.14–0.17), and then attains a saturated level (Figure 5). The sample had transformed from **BP** to **RP** at the end point of the sharp increase, as shown by the color change of sample (Figure 5). The sudden increased uptake of H_2O can be mainly attributed to the additional coordination of water to the Co^{II} ions (about 105 $cm^3 g^{-1}$ STP) and the

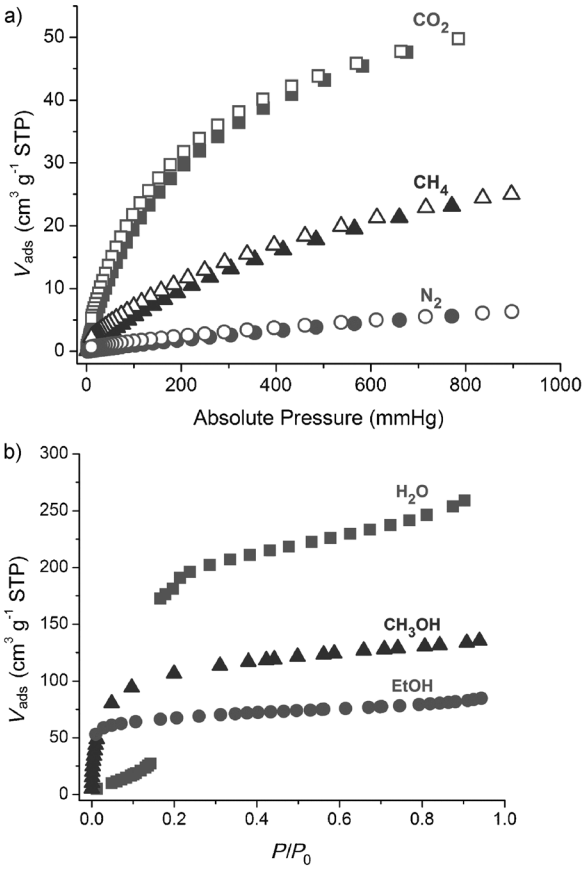

Figure 4. a) Adsorption isotherms of **BP** for CO_2, CH_4, and N_2 at 273 K. b) Vapor adsorption isotherms at 273 K.

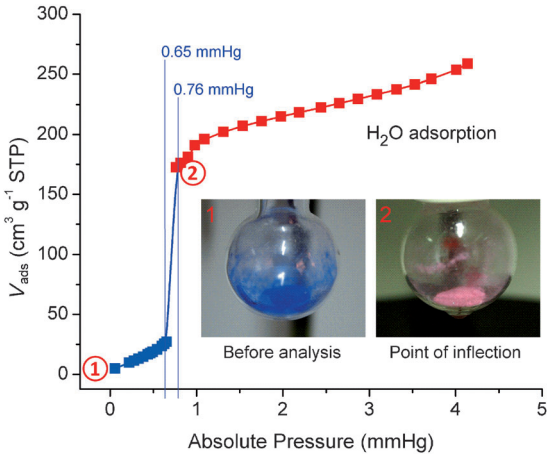

Figure 5. The SC-SC transformation during H_2O adsorption.

enhanced host–guest/guest–guest interactions between the guest H_2O molecules and cationic host **RP** framework or anionic guest pta^{2-} ligands. The opened channels that accompany structure transformation may also benefit the diffusion of H_2O molecules into the framework. The H_2O adsorption isotherm indicates that structure transformation had occurred in a narrow H_2O pressure range. This means the structure transformation as well as the gate effect can be regulated by controlling the humidity. This is also an

advantage for quantitative sensing and determination applications. Furthermore, the remarkable H_2O uptake and significant uptake differences toward H_2O and other tested gas/vapors make **BP** a good candidate for moisture remove.

In conclusion, we have successfully synthesized a Co^{II} MOF (**BP**) with ultramicropores in its structure. With the stimuli of coordinative molecules such as H_2O and NH_3, **BP** can reversibly transform to red **RP** with micropores. The reversible response to H_2O/NH_3 of this complex makes it a good candidate as a sensor material. Besides the change of framework topology, the reversible SC-SC transformation between **BP** and **RP** is accompanied by the removal/recovery of pta^{2-} ligands, which leads to a gate effect in the 1D channels. The controllable open and close of channel can encapsulate and release small guest molecules under certain conditions. As the gate effect still has some limitations, we are trying to accurately control the encapsulating capability and the sensitivity of the transformation by modifying the size and textures of the gates. Further studies are still under way.

Received: July 19, 2013
Published online: September 13, 2013

Keywords: cobalt · gate effect · metal–organic frameworks · sensors · single-crystal transformation

[1] a) D. Yuan, D. Zhao, D. J. Timmons, H.-C. Zhou, *Chem. Sci.* **2011**, *2*, 103 – 106; b) E. Y. Lee, S. Y. Jang, M. P. Suh, *J. Am. Chem. Soc.* **2005**, *127*, 6374 – 6381; c) S. Kitagawa, K. Uemura, *Chem. Soc. Rev.* **2005**, *34*, 109 – 119; d) K. Takaoka, M. Kawano, M. Tominaga, M. Fujita, *Angew. Chem.* **2005**, *117*, 2189 – 2192; *Angew. Chem. Int. Ed.* **2005**, *44*, 2151 – 2154; e) K. Hanson, N. Calin, D. Bugaris, M. Scancella, S. C. Sevov, *J. Am. Chem. Soc.* **2004**, *126*, 10502 – 10503; f) M. Albrecht, M. Lutz, A. L. Spek, G. van Koten, *Nature* **2000**, *406*, 970 – 974.

[2] a) Y. G. Huang, B. Mu, P. M. Schoenecker, C. G. Carson, J. R. Karra, Y. Cai, K. S. Walton, *Angew. Chem.* **2011**, *123*, 456 – 460; *Angew. Chem. Int. Ed.* **2011**, *50*, 436 – 440; b) J. Sun, F. Dai, W. Yuan, W. Bi, X. Zhao, W. Sun, D. Sun, *Angew. Chem.* **2011**, *123*, 7199 – 7202; *Angew. Chem. Int. Ed.* **2011**, *50*, 7061 – 7064; c) O. V. Zenkina, E. C. Keske, R. Wang, C. M. Crudden, *Angew. Chem.* **2011**, *123*, 8250 – 8254; *Angew. Chem. Int. Ed.* **2011**, *50*, 8100 – 8104; d) C.-D. Wu, W. Lin, *Angew. Chem.* **2005**, *117*, 1994 – 1997; *Angew. Chem. Int. Ed.* **2005**, *44*, 1958 – 1961; e) S. C. Sahoo, T. Kundu, R. Banerjee, *J. Am. Chem. Soc.* **2011**, *133*, 17950 – 17958; f) S. Supriya, S. K. Das, *J. Am. Chem. Soc.* **2007**, *129*, 3464 – 3465; g) P. K. Allan, B. Xiao, S. J. Teat, J. W. Knight, R. E. Morris, *J. Am. Chem. Soc.* **2010**, *132*, 3605 – 3611; h) H. Li, M. Eddaoudi, M. O'Keeffe, O. M. Yaghi, *Nature* **1999**, *402*, 276 – 279; i) A. C. McKinlay, J. F. Eubank, S. Wuttke, B. Xiao, P. S. Wheatley, P. Bazin, J. C. Lavalley, M. Daturi, A. Vimont, G. De Weireld, P. Horcajada, C. Serre, R. E. Morris, *Chem. Mater.* **2013**, *25*, 1592 – 1599.

[3] P. B. Chatterjee, A. Audhya, S. Bhattacharya, S. M. T. Abtab, K. Bhattacharya, M. Chaudhury, *J. Am. Chem. Soc.* **2010**, *132*, 15842 – 15845.

[4] a) M. C. Bernini, F. Gándara, M. Iglesias, N. Snejko, E. Gutiérrez-Puebla, E. V. Brusau, G. E. Narda, M. Á. Monge, *Chem. Eur. J.* **2009**, *15*, 4896 – 4905; b) J. Y. Lee, S. Y. Lee, W. Sim, K.-M. Park, J. Kim, S. S. Lee, *J. Am. Chem. Soc.* **2008**, *130*, 6902 – 6903; c) J.-P. Zhang, Y.-Y. Lin, W.-X. Zhang, X.-M. Chen, *J. Am. Chem. Soc.* **2005**, *127*, 14162 – 14163.

[5] a) J. Fu, H. Li, Y. Mu, H. Hou, Y. Fan, *Chem. Commun.* **2011**, *47*, 5271 – 5273; b) K. Raatikainen, K. Rissanen, *Chem. Sci.* **2012**, *3*, 1235 – 1239; c) Y. Han, H. Xu, Y. Liu, H. Li, H. Hou, Y. Fan, S. R. Batten, *Chem. Eur. J.* **2012**, *18*, 13954 – 13958; d) J.-J. Jiang, L. Li, M.-H. Lan, M. Pan, A. Eichhofer, D. Fenske, C.-Y. Su, *Chem. Eur. J.* **2010**, *16*, 1841 – 1848; e) C. Massera, M. Melegari, E. Kalenius, F. Ugozzoli, E. Dalcanale, *Chem. Eur. J.* **2011**, *17*, 3064 – 3068; f) I.-H. Park, S. S. Lee, J. J. Vittal, *Chem. Eur. J.* **2013**, *19*, 2695 – 2702; g) S. Hu, K.-H. He, M.-H. Zeng, H.-H. Zou, Y.-M. Jiang, *Inorg. Chem.* **2008**, *47*, 5218 – 5224; h) H. J. Choi, M. P. Suh, *J. Am. Chem. Soc.* **2004**, *126*, 15844 – 15851; i) L. Dobrzańska, G. O. Lloyd, H. G. Raubenheimer, L. J. Barbour, *J. Am. Chem. Soc.* **2006**, *128*, 698 – 699; j) D. Liu, J.-P. Lang, B. F. Abrahams, *J. Am. Chem. Soc.* **2011**, *133*, 11042 – 11045; k) M.-H. Zeng, Q.-X. Wang, Y.-X. Tan, S. Hu, H.-X. Zhao, L.-S. Long, M. Kurmoo, *J. Am. Chem. Soc.* **2010**, *132*, 2561 – 2563; l) Y.-Q. Chen, G.-R. Li, Z. Chang, Y.-K. Qu, Y.-H. Zhang, X.-H. Bu, *Chem. Sci.* **2013**, *4*, 3678 – 3682.

[6] a) C.-L. Chen, A. M. Goforth, M. D. Smith, C.-Y. Su, L. H.-C. zur, *Angew. Chem.* **2005**, *117*, 6831 – 6835; *Angew. Chem. Int. Ed.* **2005**, *44*, 6673 – 6677; b) Z. Su, M. Chen, T.-a. Okamura, M.-S. Chen, S.-S. Chen, W.-Y. Sun, *Inorg. Chem.* **2011**, *50*, 985 – 991.

[7] Crystal and refinement information: **BP**⊃DMF: monoclinic, *C*2/*c*, $a = 21.665(9)$, $b = 27.475(11)$, $c = 14.277(6)$ Å, $\beta = 103.073(5)°$, $V = 8278(6)$ Å^3, $T = 113$ K, $Z = 4$, $R_1 = 0.1432$, $wR_2 = 0.3008$, GOF = 1.201; **RP**-H_2O: monoclinic, *C*2/*c*, $a = 23.020(13)$, $b = 28.032(16)$, $c = 12.506(7)$ Å, $\beta = 100.389(7)°$, $V = 7938(8)$ Å^3, $T = 113$ K, $Z = 4$, $R_1 = 0.1020$, $wR_2 = 0.3236$, GOF = 1.099; **BP**-brb: monoclinic, *C*2/*c*, $a = 21.719(4)$, $b = 27.620(6)$, $c = 14.255(3)$ Å, $\beta = 103.18(3)°$, $V = 8326(3)$ Å^3, $T = 113$ K, $Z = 4$, $R_1 = 0.1345$, $wR_2 = 0.3784$, GOF = 1.186. CCDC 933244 (**BP**⊃DMF), 933245 (**RP**-H_2O), and 933243 (**BP**-brb) contain the supplementary crystallographic data for this paper. These data can be obtained free of charge from The Cambridge Crystallographic Data Centre via www.ccdc.cam.ac.uk/data_request/cif.

[8] X. N. Cheng, W. X. Zhang, Y. Y. Lin, Y. Z. Zheng, X. M. Chen, *Adv. Mater.* **2007**, *19*, 1494 – 1498.

[9] a) M. O' Keeffe, Reticular Chemistry Structure Resource (http://rcsr.anu.edu.au/); b) V. A. Blatov, A. P. Shevchenko, V. N. Serezhkin, *Russ. J. Coord. Chem.* **1999**, *25*, 453 – 465; http://www.topos.ssu.samara.ru.

[10] a) L. G. Beauvais, M. P. Shores, J. R. Long, *J. Am. Chem. Soc.* **2000**, *122*, 2763 – 2772; b) J. A. Real, E. Andrés, M. C. Muñoz, M. Julve, T. Granier, A. Bousseksou, F. Varret, *Science* **1995**, *268*, 265 – 267.

[11] a) R. Kitaura, K. Seki, G. Akiyama, S. Kitagawa, *Angew. Chem.* **2003**, *115*, 444 – 447; *Angew. Chem. Int. Ed.* **2003**, *42*, 428 – 431; b) R. Kitaura, K. Fujimoto, S.-i. Noro, M. Kondo, S. Kitagawa, *Angew. Chem.* **2002**, *114*, 141 – 143; *Angew. Chem. Int. Ed.* **2002**, *41*, 133 – 135; c) J.-P. Zhang, Y.-B. Zhang, J.-B. Lin, X.-M. Chen, *Chem. Rev.* **2012**, *112*, 1001 – 1033; d) H. J. Choi, M. Dinca?, J. R. Long, *J. Am. Chem. Soc.* **2008**, *130*, 7848 – 7850; e) C. Gücüyener, J. van den Bergh, J. Gascon, F. Kapteijn, *J. Am. Chem. Soc.* **2010**, *132*, 17704 – 17706; f) L. Hamon, P. L. Llewellyn, T. Devic, A. Ghoufi, G. Clet, V. Guillerm, G. D. Pirngruber, G. Maurin, C. Serre, G. Driver, W. v. Beek, E. Jolimaitre, A. Vimont, M. Daturi, G. Férey, *J. Am. Chem. Soc.* **2009**, *131*, 17490 – 17499; g) J.-P. Zhang, X.-M. Chen, *J. Am. Chem. Soc.* **2009**, *131*, 5516 – 5521; h) A. Kondo, H. Noguchi, S. Ohnishi, H. Kajiro, A. Tohdoh, Y. Hattori, W.-C. Xu, H. Tanaka, H. Kanoh, K. Kaneko, *Nano Lett.* **2006**, *6*, 2581 – 2584; i) J. Brown, B. L. Henderson, M. D. Kiesz, A. C. Whalley, W. Morris, S. Grunder, H. Deng, H. Furukawa, J. I. Zink, J. F. Stoddart, O. M. Yaghi, *Chem. Sci.* **2013**, *4*, 2858 – 2864.

